Investigation of the corrosion resistance properties of a new synthesized Schiff base compound on XC48 steel in two acidic media: 1 M HCl and 0.5 M H_2SO_4

H. Belagra,[1,2] F. Benghanem,[2] R. Yekhlef [2,3] and D. Belfennache[3]*

[1]*Department of Chemistry, Faculty of Sciences, University Mohamed Boudiaf of M'Sila, University of M'Sila, University Pole, Bordj Bou Arreridj road, M'Sila 28000, Algeria*
[2]*Laboratory of Electrochemistry, molecular engineering and Redox Catalysis (LEIMCR), University Sétif-1, Setif 19000, Algeria*
[3]*Research Center in Industrial Technologies CRTI, P.O. Box 64, Cheraga, 16014 Algiers, Algeria*
**E-mail: houria.belagra@univ-msila.dz*

Abstract

Schiff bases represent a crucial group of widely used chemical compounds with various applications across multiple domains. This research investigates the corrosion inhibition properties of a newly developed Schiff base, bis(3-methoxysalicylidene)-4,4′-diiminodiphenyl methane (BMDDM), on XC48 steel in 1 M hydrochloric acid and 0.5 M sulfuric acid using electrochemical methods, specifically potentiodynamic polarization and impedance spectroscopy. The study varied two parameters: concentration (ranging from 10^{-6} to 10^{-3} M) and temperature (from 30 to 60°C). To understand the mechanism of action of this Schiff base, we calculated and analyzed several thermodynamic parameters related to the activation and adsorption processes (E_a, ΔH_a, ΔG_{ads}, and ΔS_a). The optimal concentration of 10^{-3} M yielded inhibition efficiencies of 89.33% in 1 M hydrochloric acid and 88.37% in 0.5 M sulfuric acid. The findings indicated that the Schiff base acts as a mixed inhibitor, with the inhibition mechanism conforming to the Langmuir isotherm in both acidic environments. The calculated ΔG_{ads} values suggest that the inhibitor undergoes both chemisorption and physisorption in HCl and H_2SO_4. In terms of temperature effects, the highest inhibition efficiency recorded was 78.45% at 40°C in hydrochloric acid and 76.05% at 30°C in sulfuric acid. Scanning electron microscopy (SEM) images confirmed the formation of organic molecules that create a stable and insoluble protective layer on the surface of XC48 carbon steel.

Received: December 17, 2024. Published: January 18, 2025 doi: 10.17675/2305-6894-2025-14-1-5

Keywords: *corrosion, Schiff base, inhibitor, XC48 steel, acidic medium.*

1. Introduction

A real development of modern industry is essentially based on the quality of finished products. Today, manufacturing engineers must be equipped to address numerous inquiries to efficiently produce parts that meet quality standards. This can be achieved by mastering

technology and strengthening it through scientific research [1–3]. Corrosion of metals is a prevalent issue in the industrial sector, often leading to significant safety concerns [4]. Corrosion results from a chemical and/or physical action of a metal or alloy with its environment [5]. The consequences are substantial across multiple domains, particularly in industry. Frequent occurrences include production shutdowns, replacement of corroded components, serious accidents, and pollution risks, all of which can lead to significant economic implications. In terms of protection, the use of corrosion inhibitors is an essential strategy for preserving metals and alloys from corrosion [6–8]. The purpose may be either for permanent protection of the component, necessitating meticulous care, or for temporary protection, especially when the component is highly susceptible to corrosion or subjected to a highly aggressive environment [9, 10].

Acid solutions are widely employed in numerous industrial applications, including acid cleaning and the removal of deposits such as scale, rust, and bacterial buildup [11–13]. The corrosive properties of these acid solutions highlight the importance of using corrosion inhibitors, which are vital for reducing the degradation of metallic materials during industrial processes [14]. Research on the protection of steels from corrosion has shown that many effective inhibitors are organic compounds containing elements such as nitrogen, oxygen, and sulfur. Among these, Schiff bases have demonstrated considerable efficacy in acidic environments. These inhibitors work by forming covalent bonds with metals, primarily through the adsorption onto metal surfaces. This process is facilitated by the lone pair of electrons on the nitrogen atom and the presence of π bonds, allowing for strong interactions that enhance the protective barrier against corrosion [15–17].

In order to contribute to the various research relating on the one hand to the corrosion of steels and their inhibition in the various solutions encountered in the industrial sector. In our research, we investigated the inhibitory efficacy of a newly synthesized Schiff base, bis(3-methoxysalicylidene)-4,4′-diiminodiphenylmethane, against the corrosion of XC48 steel in 1 M hydrochloric acid and 0.5 M sulfuric acid environments. We employed electrochemical techniques, specifically potentiodynamic polarization and impedance spectroscopy, to assess the performance of this Schiff base as a corrosion inhibitor. Our findings contribute to the understanding of how this compound can effectively protect steel in aggressive acidic conditions.

2. Experimental

2.1. Metal specimen

The working electrode used in our study is XC48 steel, which is primarily composed of iron, along with several alloying elements that enhance its mechanical and corrosion-resistant properties. The specific composition of elements other than iron in XC48 steel is provided in the following Table 1. This is an unalloyed steel which is generally used in the manufacture of mold parts subjected to shocks and requiring good resistance: axles, gears, worm screws, bearings, pinions, bolts, forging (levers, shafts).

Table 1. The composition of XC48 steel.

Element	C	S	P	Mn	Cr	Si
Composition (%)	0.45–0.50	0.005	0.02	0.35–0.45	0.9–3.7	0.7–0.9

2.2. Solution

The 1.0 M HCl and 0.5 M H_2SO_4 solution was prepared by diluting of a reagent grade HCl (37%) and H_2SO_4 (98%). The inhibitor bis(3-methoxysalicylidene)-4,4′-diminodiphenyl-methane (PNM) (Figure 1) was synthesized. The range of concentrations used for the BMDDM inhibitor is $5{\cdot}10^{-3}$ to $1.0{\cdot}10^{-6}$ M.

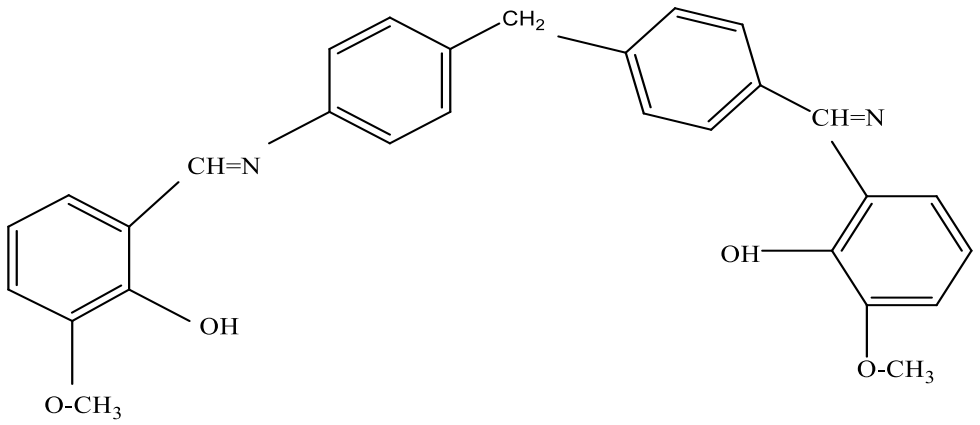

Figure 1. Schematic of the molecular structure of bis-(3-methoxy-salicylidene)-4,4-di-aminophenylmethane used in this work.

2.3. Electrochemical investigations

This work was carried out using an experimental device consisting of a VOLTALAB type PGZ 301, allowing electrochemical measurements, assisted by a DELL type microcomputer, connected to an appropriate interface, equipped with software (VoltaMaster 4) allowing the acquisition and processing of data as well as the determination of the various electrochemical parameters. The electrochemical experiments were conducted in a thermostated cylindrical glass measuring cell with a capacity of 100 mL. This setup is equipped with a simple ground cover featuring five holes, which allows for the precise positioning of our working electrodes in a fixed and reproducible manner.

The configuration of the electrodes is as follows: working electrode: a cylindrical piece of XC48 steel with a diameter of 6 mm; reference electrode: an Ag/AgCl reference electrode, which maintains a constant potential of 140 mV versus the normal hydrogen electrode (NHE). In our electrochemical setup, we utilized a platinum counter electrode with a surface area of 1 cm². This counter electrode was strategically positioned near the working electrode (the XC48 steel) to ensure a homogeneous electric field throughout the cell. The steel surface is initially stripped by mechanical polishing with abrasive paper of different grain sizes, then rinsed with distilled water. The electrode thus has a very smooth surface allowing

reproducible results. Since the steady state is slow to establish in most cases, the plotting of the current-voltage curves is delicate. For this reason, the choice of the scanning speed can be rigorous. After several tests and according to the literature [14], we worked with a speed of 2 mV/s. The plotting of the polarization curves was carried out in a potential range corresponding to –800 mV to –200 mV with respect to Ag/AgCl.

2.4. Surface analyses

We examined the surface features of our steel samples using a scanning electron microscope (SEM) after exposing them to 1.0 M HCl and 0.5 M H_2SO_4 solutions, both with and without the BMDDM inhibitor. The samples were submerged for 24 hours before analysis.

3. Results and Discussions

This section focuses on investigating the effectiveness of a novel Schiff base compound in preventing corrosion of XC48 steel in acidic environments, specifically 1 M HCl and 0.5 M H_2SO_4. This study is carried out using two electrochemical techniques namely dynamic polarization and impedancemetry by varying two parameters: the concentration from 10^{-6} to 10^{-3} M and the temperature from 30 to 60°C. Thus, to determine the mode of action of this Schiff base, we calculated and commented on some thermodynamic values of the activation and adsorption process (E_a, ΔH_a, ΔG_{ads} and ΔS_a).

3.1. Study of the inhibitory power of the Schiff base

3.1.1. Effect of concentration

Our primary goal was to assess the inhibitory capacity of the Schiff base in acidic media (1 M HCl and 0.5 M H_2SO_4), both with and without varying concentrations of the inhibitor.

3.1.1.1. Results of impedancemetry

Figure 2 depicts Nyquist diagrams obtained at 25°C for XC48 steel immersed in 1 M HCl and 0.5 M H_2SO_4 media, both without and with varying concentrations of the investigated Schiff base.

The diameters of the Nyquist diagrams in Figure 2 are influenced by the concentration of the Schiff base. As the concentration of the Schiff base increases, the impedance of the XC48 steel electrode in the acidic media also increases. This indicates that the inhibitor molecules are covering more of the metal surface, leading to a higher rate of inhibition. Tables 2 and 3 summarize the electrochemical parameters derived from the impedance data, including polarization resistance (R_p), which is calculated from the impedance difference at low and high frequencies. The values of the double layer capacitance (C_{dl}) are obtained from the following equation:

$$f(-Z_{max}) = \frac{1}{2\pi C_{dl} R_p} \quad (1)$$

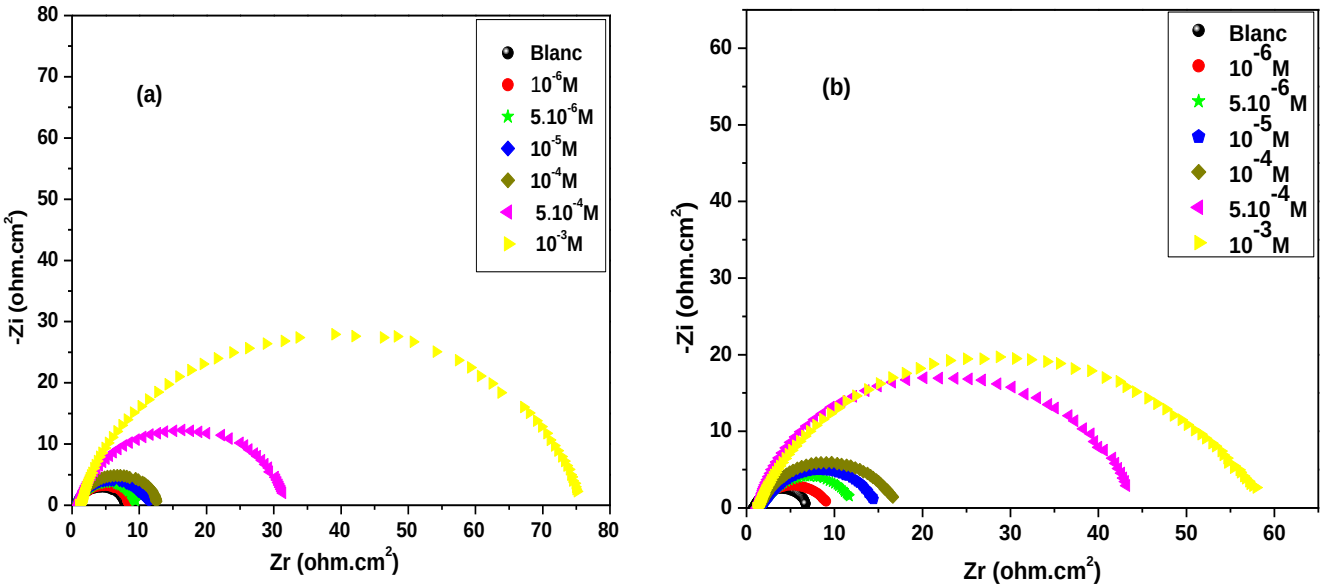

Figure 2. Nyquist diagrams of XC48 steel (a) in HCl and (b) in H_2SO_4 in the absence and presence of different concentrations of the Schiff base after 30 min of immersion and at room temperature.

The inhibition efficiency (*IE*%) is calculated from equation (2):

$$IE\% = \frac{R_{p,inh} - R_p}{R_{p,inh}} \times 100 \quad (2)$$

where R_p and $R_{p,inh}$ are the values of the polarization resistance in the absence and presence of the Schiff base respectively.

Table 2. Electrochemical parameters of impedancemetry for XC48 steel in 1 M HCl in the absence and presence of different concentrations of the Schiff base at room temperature.

C(M) HCl	R_p (Ohm·cm^2)	R_s (Ohm·cm^2)	C_{dl} (μF·cm^{-2})	*IE*%
0	8.01	0.88	1031	0
10^{-6}	8.42	0.96	689.6	4.98
$5{\cdot}10^{-6}$	9.50	0.85	591.9	15.78
10^{-5}	11.50	0.74	564.8	30.43
10^{-4}	12.54	0.85	421.0	36.20
$5{\cdot}10^{-4}$	31.33	1.03	183.4	74.46
10^{-3}	75.00	1.13	134.6	89.33

Table 3. Electrochemical parameters of impedancemetry for XC48 steel in 0.5 M H_2SO_4 in the absence and presence of different concentrations of Schiff base at room temperature.

***C*(M) H_2SO_4**	***R*$_p$ (Ohm·cm^2)**	***R*$_s$ (Ohm·cm^2)**	***C*$_{dl}$ (µF·cm^{-2})**	***IE*%**
0	6.73	0.87	580.4	0
10^{-6}	9.07	1.29	547.4	25.79
$5\cdot10^{-6}$	11.70	1.57	528.4	42.47
10^{-5}	14.42	1.58	317.8	53.32
10^{-4}	16.62	1.36	299.1	59.50
$5\cdot10^{-4}$	43.21	1.26	276.1	84.42
10^{-3}	57.91	1.05	149.5	88.37

Analyzing the data in Tables 2 and 3 revealed that the presence of the inhibitor leads to a decrease in the double layer capacitance (C_{dl}) and a corresponding increase in the charge transfer resistance (Figure 3). This observation suggests that the inhibitor molecules are adsorbing onto the steel surface, forming a stable protective layer. As the amount of adsorbed inhibitor increases, the thickness of this protective layer grows, resulting in a decrease in the double layer capacitance.

The inhibition rates increase with increasing concentration and reach values of 89.33% in 1 M HCl and 88.37% in 0.5 M H_2SO_4 at 10^{-3} M.

3.1.1.2. Potentiodynamic polarization results

Figure 3 presents the polarization curves of XC48 steel in 1 M HCl and 0.5 M H_2SO_4 acid solutions, both before and after the addition of the Schiff base at different concentrations.

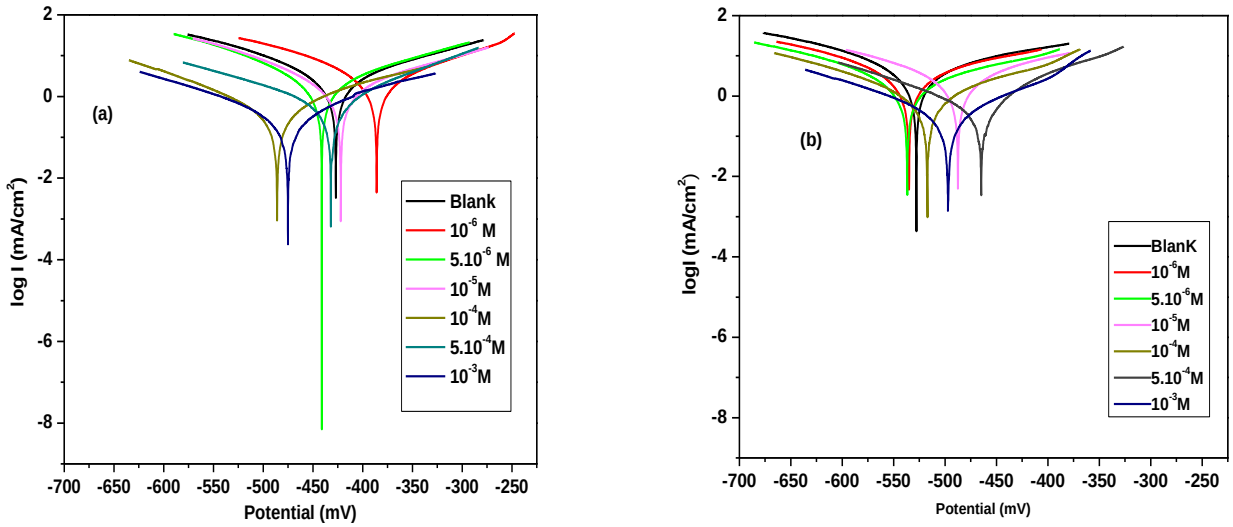

Figure 3. Tafel curves of XC48 steel in both media: (a) in HCl and (b) in H_2SO_4 without and with addition of different concentrations of Schiff base after 30 min of immersion at room temperature.

From the Tafel lines shown in Figure 3, we were able to determine various electrochemical characteristics. Tables 4 and 5 present the corrosion current densities (i_{corr}), corrosion potential (E_{corr}), cathodic and anodic Tafel slopes (β_c and β_a), and inhibition efficiency for different concentrations of the Schiff base in both 1 M HCl and 0.5 M H_2SO_4 media. The inhibition efficiency is defined as follows:

$$IE\% = \frac{i_{corr^\circ} - i_{corr,inh}}{i_{corr^\circ}} \times 100 \quad (3)$$

where: i_{corr° and $i_{corr,inh}$ represent the values of current densities of XC48 steel immersed in acidic media respectively without and with the addition of Schiff base.

Based on the data presented in Tables 4 and 5, we can draw the following conclusions:

- The corrosion potential does not exhibit a consistent pattern as the Schiff base concentration changes.
- The inhibitor's mixed nature is evident from the altered slopes of the cathodic and anodic Tafel lines.
- The addition of the Schiff base results in a reduction of current densities. The corrosion rate (icorr) decreases as the concentration of the ligand increases, suggesting that the inhibition process is driven by the adsorption of the Schiff base onto the steel surface. The optimal concentration for achieving the highest inhibition efficiency is 10^{-3} M (Tables 4 and 5).
- The inhibition efficiency shows an increasing trend as the Schiff base concentration increases.

From all these remarks we conclude that this product inhibits the corrosion of XC48 steel in the study media and that it is of mixed type. These good inhibitory properties can be due to the adsorption of the Schiff base molecules on the surface of the XC48 steel. In summary, the results obtained in 1 M HCl and 0.5 M H_2SO_4 from the electrochemical techniques used are consistent. The determined inhibition rates are close and evolve in the same way.

3.1.2. Effect of temperature

Temperature plays a crucial role in corrosion processes. Generally, as the temperature increases, the corrosion rate also increases. This temperature dependency can significantly alter the effectiveness of corrosion inhibitors.

3.1.2.1. Study by electrochemical impedance spectroscopy

To investigate how temperature impacts the formation of the inhibitory film and to validate our previous findings, we studied the influence of temperature on the electrochemical behavior of XC48 steel using electrochemical impedance spectroscopy (EIS). We plotted the electrochemical impedance diagrams for XC48 steel in both 1 M HCl and 0.5 M H_2SO_4 solutions, both in the absence and presence of the Schiff base (Figure 4).

Table 4. Electrochemical parameters and corrosion inhibition efficiency for XC48 steel in HCl, without and with different concentrations of the Schiff base at room temperature.

C(M) HCl	$-E_{corr}$ (mV/Ag/AgCl)	i_{corr} (mA·cm^{-2})	β_a (mV·Dec^{-1})	$-\beta_c$ (mV·Dec^{-1})	τ_{corr} (mm/an)	R_p (Ohm·cm^2)	*IE*%	θ
0	427.0	2.47	149.9	123.5	28.9	9.47	–	–
10^{-6}	386.0	2.15	127.3	114.4	25.18	10.04	12.95	0.12
$5\cdot10^{-6}$	441.1	2.04	145.8	116.6	23.93	11.81	17.40	0.17
10^{-5}	422.0	1.62	151.6	116.4	18.95	17.75	34.41	0.34
10^{-4}	486.0	0.71	173.6	130.1	8.35	58.15	71.25	0.71
$5\cdot10^{-4}$	432.2	0.67	110.8	147.2	7.87	65.05	72.87	0.72
10^{-3}	475.1	0.35	148.5	141.0	4.12	111.47	85.82	0.85

Table 5. Electrochemical parameters and corrosion inhibition efficiency of XC48 steel in H_2SO_4 without and with addition of different concentrations of the Schiff base at room temperature.

C(M) HCl	$-E_{corr}$ (mV/Ag/AgCl)	i_{corr} (mA·cm^{-2})	β_a (mV·Dec^{-1})	$-\beta_c$ (mV·Dec^{-1})	τ_{corr} (mm/an)	R_p (Ohm·cm^2)	*IE*%	θ
0	427.9	4.95	244.9	169.5	57.89	7.65	–	–
10^{-6}	535.1	3.45	209.9	153.4	40.56	9.54	30.30	0.30
$5\cdot10^{-6}$	536.9	2.24	198.5	136.8	26.20	10.08	54.74	0.54
10^{-5}	487.4	2.14	146.5	129.7	25.07	16.18	56.76	0.56
10^{-4}	517.3	1.20	160.6	149.3	14.04	31.90	75.75	0.75
$5\cdot10^{-4}$	464.7	0.58	81.2	130.1	6.86	33.60	88.28	0.88
10^{-3}	497.5	0.32	103.7	116.5	3.85	39.56	93.53	0.93

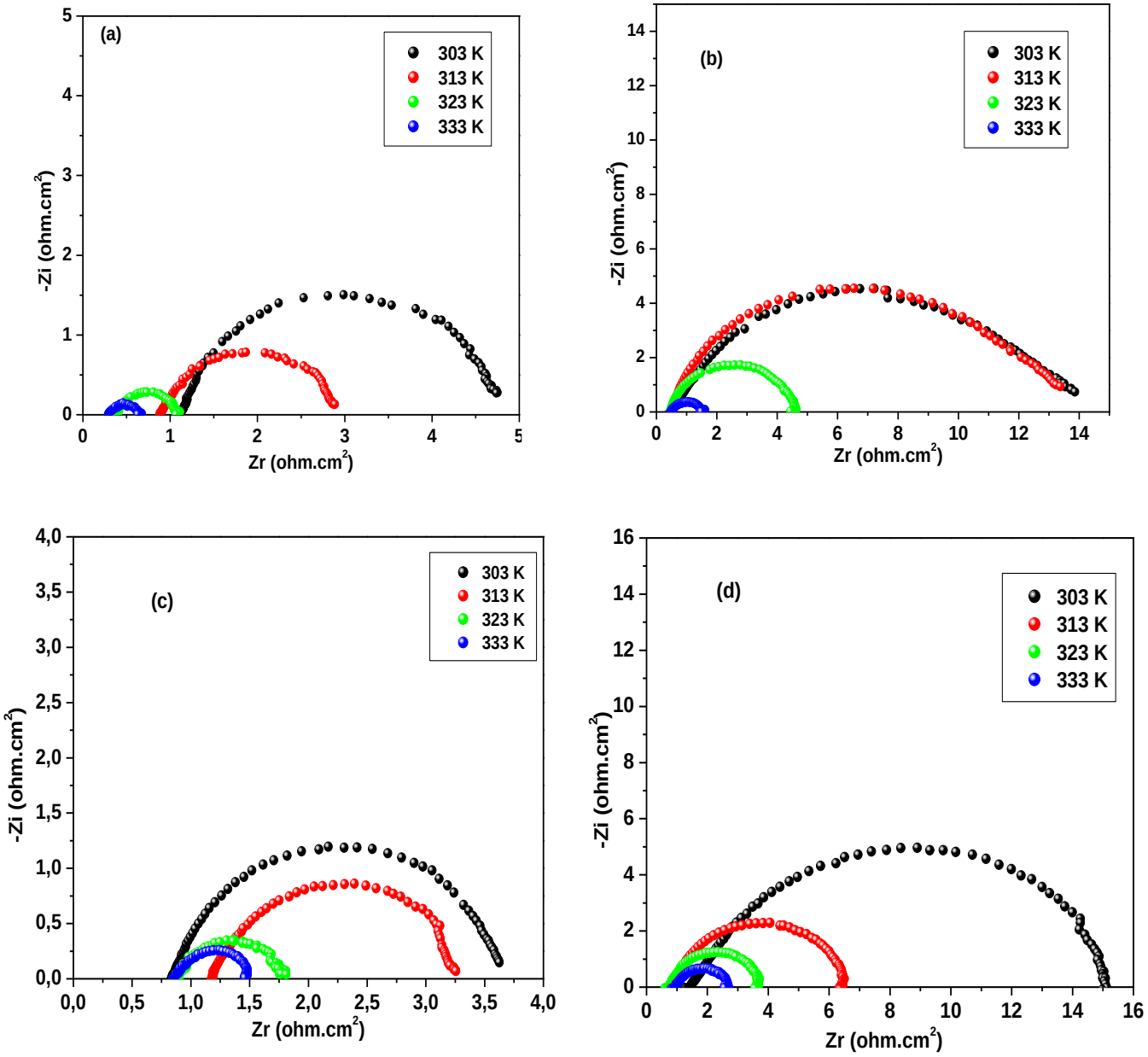

Figure 4. Nyquist diagrams of XC48 steel as a function of temperature in HCl medium: (a) in the absence of Schiff base, (b) in the presence of 10^{-3} M Schiff base and in H_2SO_4 medium: (c) in the absence of Schiff base, (d) in the presence of 10^{-3} M Schiff base after 30 min of immersion.

The Nyquist diagrams, shown in Figure 4, provided us with the necessary data to determine several electrochemical parameters. These parameters are summarized in Tables 6 and 7.

Table 6. Electrochemical parameters and corrosion inhibitory efficiency of XC48 steel in 1 M HCl in the absence and presence of 10^{-3} M Schiff base as a function of temperature.

	T **(K)**	R_t **(Ohm·cm²)**	R_s **(Ohm·cm²)**	C_{dl} **(μF·cm⁻²)**	***IE*%**	**θ**
Without inhibitor (HCl blank)	303	4.75	1.11	1.36	–	–
	313	2.88	0.89	1.76	–	–
	323	1.11	0.37	3.90	–	–
	333	0.67	0.29	9.30	–	–
With inhibitor (10^{-3} M)	303	13.87	0.52	0.79	65.75	0.65
	313	13.37	0.46	0.87	78.45	0.78
	323	4.60	0.44	1.51	75.86	0.75
	333	1.55	0.47	2.60	56.77	0.56

Table 7. Electrochemical parameters and corrosion inhibitory efficiency of XC48 steel in 0.5 M H_2SO_4 in the absence and presence of 10^{-3} M Schiff base as a function of temperature.

	T **(K)**	R_t **(Ohm·cm²)**	R_s **(Ohm·cm²)**	C_{dl} **(μF·cm⁻²)**	***IE*%**	**θ**
Without inhibitor (H_2SO_4 blank)	303	3.62	0.84	0.90	–	–
	313	3.25	1.17	1.27	–	–
	323	1.81	0.88	3.47	–	–
	333	1.45	0.84	1.78	–	–
With inhibitor (10^{-3} M)	303	15.12	1.54	0.41	76.05	0.76
	313	6.45	0.90	0.44	49.61	0.49
	323	3.61	0.75	0.47	49.86	0.49
	333	2.69	0.94	1.02	46.09	0.46

Analyzing the data in Table 7, we observed that the charge transfer resistance decreases as the temperature increases from 30°C to 60°C. Additionally, the inhibition efficiency generally decreases with increasing temperature.

3.1.2.2. Potentiodynamic polarization study

The Tafel curves in the absence and presence of the Schiff base at different temperatures in the two media HCl 1 M and H_2SO_4 0.5 M with a concentration 10^{-3} M are presented in Figure 5.

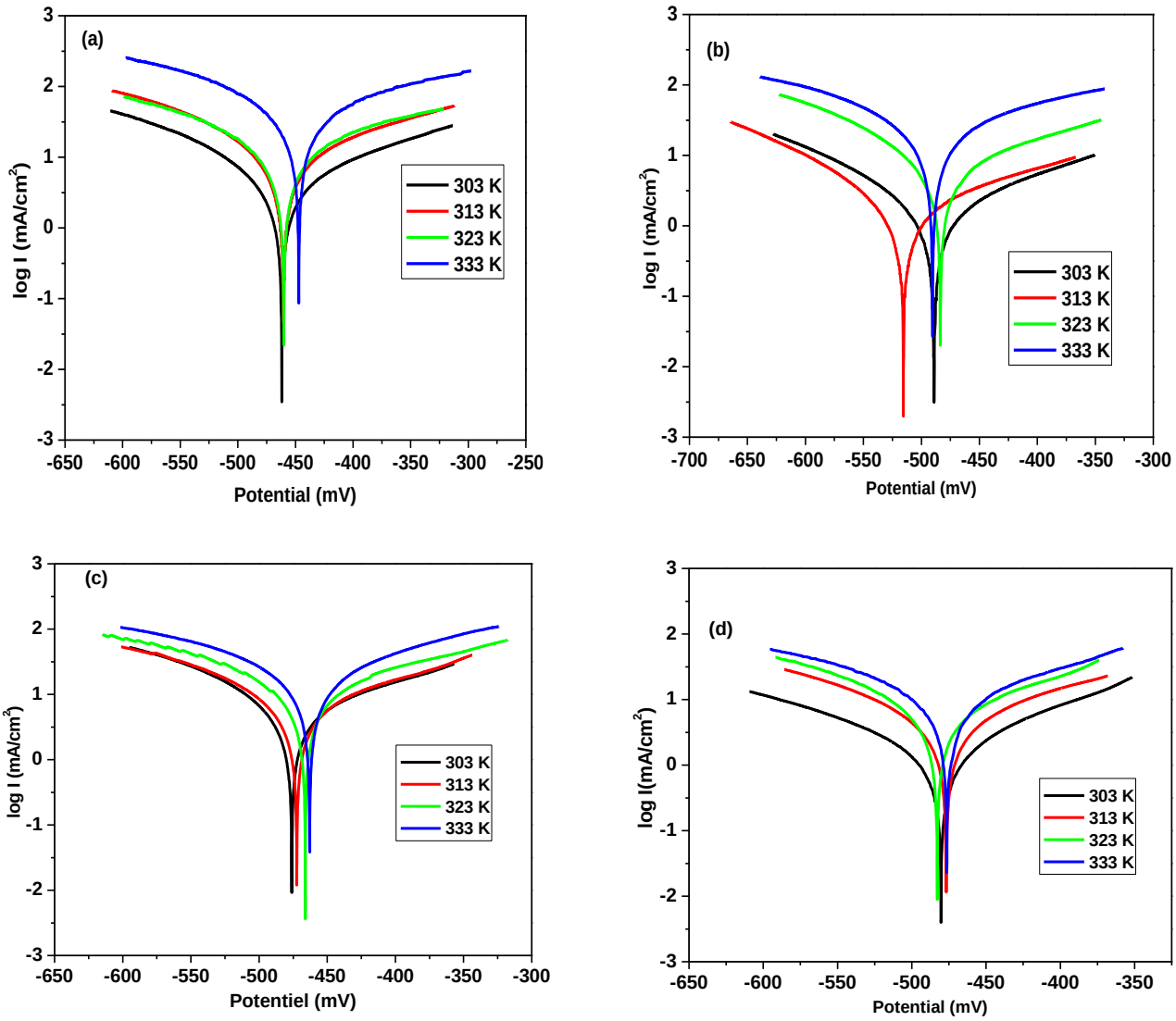

Figure 5. Tafel curves of XC48 steel as a function of temperature in HCl medium: (a) in the absence of Schiff base, (b) in the presence of 10^{-3} M Schiff base and in H_2SO_4 medium: (c) in the absence of the Schiff base, (d) in the presence of 10^{-3} M Schiff base after 30 min of immersion.

The corrosion parameters and the inhibition efficiency for the different temperatures are gathered in Tables 7 and 8.

Table 8. Electrochemical parameters and corrosion inhibitory efficiency of XC48 steel in 1 M HCl without and with the addition of 10^{-3} M Schiff base as a function of temperature.

	T (K)	$-E_{corr}$ (mV/Ag/AgCl)	i_{corr} (mA·cm^{-2})	β_a (mV·Dec^{-1})	$-\beta_c$ (mV·Dec^{-1})	τ_{corr} (mm/an)	R_p (Ohm·cm^2)	IE%	θ
Without inhibitor (HCl blank)	303	461.9	4.71	190.8	146.6	55.17	7.16	–	–
	313	460.3	10.72	212	159.6	125.4	1.75	–	–
	323	460.1	15.20	274.1	196.2	177.8	2.67	–	–
	333	447.1	56.42	339.6	219.1	660	0.72	–	–
With inhibitor (10^{-3} M)	303	488.9	1.74	181.9	129.9	20.44	12.4	63	0.63
	313	515.4	2.36	235.1	132.9	27.63	7.42	78	0.78
	323	483.6	6.67	205.1	131.8	78.12	3.57	56	0.56
	333	490.4	26.4	279.9	189	308.8	1.5	53	0.53

Table 9. Electrochemical parameters and corrosion inhibitory efficiency of XC48 steel in 0.5 M H_2SO_4 without and with addition of 10^{-3} M Schiff base as a function of temperature.

	T (K)	$-E_{corr}$ (mV/Ag/AgCl)	i_{corr} (mA·cm^{-2})	β_a (mV·Dec^{-1})	$-\beta_c$ (mV·Dec^{-1})	τ_{corr} (mm/an)	R_p (Ohm·cm^2)	$IE\%$	θ
Without inhibitor (H_2SO_4 blank)	303	476	5.41	167.4	109.1	63.38	3.88	–	–
	313	472.3	6.02	204.6	129.2	107.7	3.65	–	–
	323	466.1	12.71	211.4	152.2	148.6	2.45	–	–
	333	462.9	19.78	178.8	167.6	231.3	1.47	–	–
With inhibitor (10^{-3}M)	303	480.3	1.76	121.6	144.2	20.59	12.77	67.5	0.67
	313	476.8	5.2	171.9	144.3	50.77	5.6	13.6	0.13
	323	482.9	6.33	180.7	118.5	74.06	3.85	50.2	0.50
	333	476.5	9.63	155.8	130.4	112.7	2.34	51.3	0.51

We observed that the current densities increase with increasing temperature in both media. Additionally, the slopes of the cathodic and anodic Tafel lines vary with temperature. The inhibition rate generally shows a slight decrease with increasing temperature.

It is known that the decrease in inhibition efficiency at higher temperatures is related to physisorption. The Schiff base has an inhibitory efficiency of about 78% at T=313 K in 1 M HCl medium and 67% in 0.5 M H_2SO_4. The Arrhenius equation (4) gives the dependence of the corrosion rate on temperature.

$$i_{corr} = k \exp\left(\frac{-E_a}{RT}\right) \tag{4}$$

where E_a represents the activation energy of the hydrogen ion discharge, R is the ideal gas constant, T is the temperature and k is the pre-exponential factor.

We determined the thermodynamic characteristics of the corrosion reaction, specifically the activation energy (E_a), entropy of activation (ΔS_a), and enthalpy of activation (ΔH_a), using the Arrhenius equation and the alternative formulation known as the transition state equation (5):

$$i_{corr} = \frac{RT}{Nh} \exp\left(\frac{\Delta S_a}{R}\right) \exp\left(\frac{-\Delta H_a}{RT}\right) \tag{5}$$

where h is the Plank constant and N is the Avogadro number.

Figures 6 and 7 present the Arrhenius diagrams for a temperature range of 303–333 K. The values of the activation energy (E_a) and the pre-exponential factor (k) are determined from Figure 6.

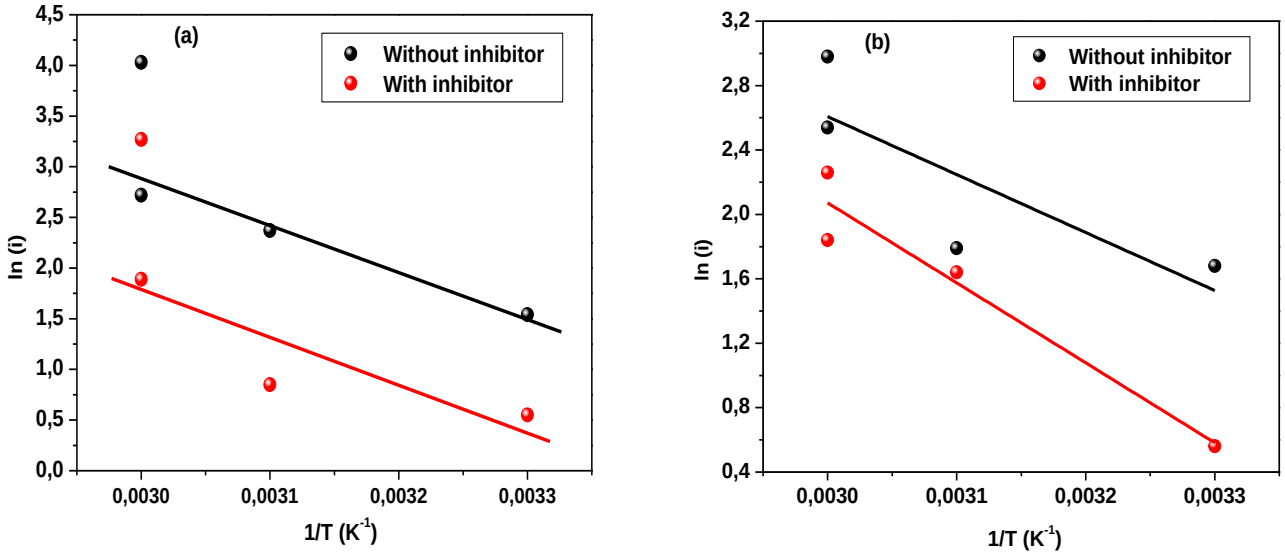

Figure 6. Variation of ln(i) as a function of the inverse of the temperature in the absence and presence of the Schiff base 10^{-3} M.

The thermodynamic parameters obtained from equations (4, 5) are grouped in Table 10.

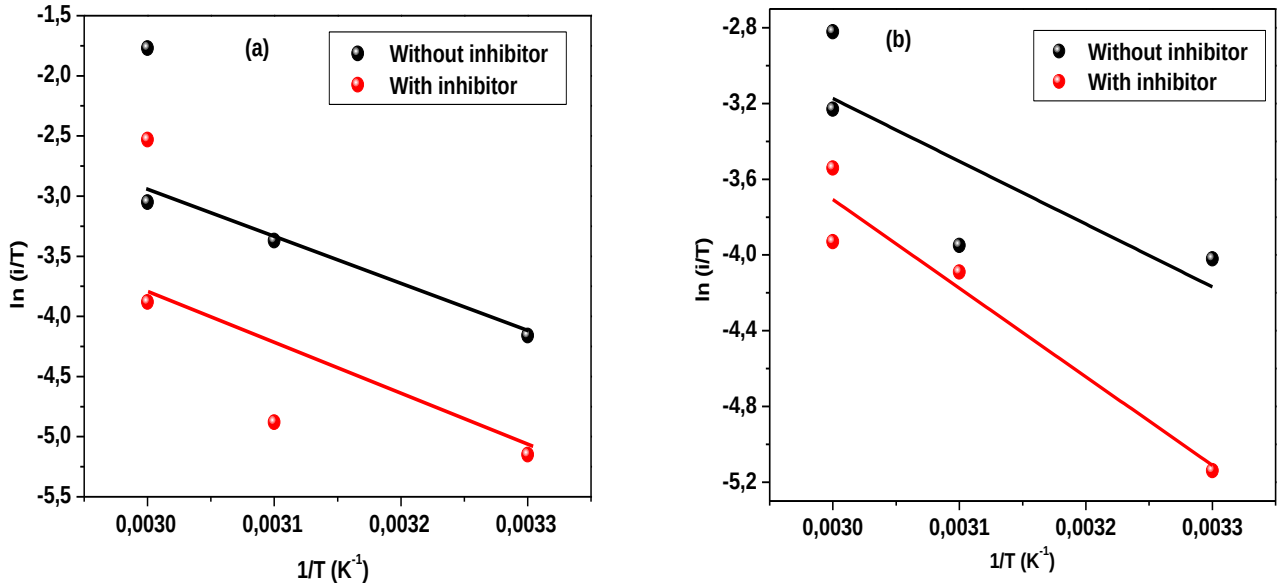

Figure 7. Variation of ln(*i*/*T*) as a function of the inverse of the temperature in the absence and presence of the Schiff base 10^{-3} M.

Table 10. Thermodynamic characteristics of the adsorption of the Schiff base on XC48 steel in the two media 1 M HCl and 0.5 M H_2SO_4.

		$-E_a$ (kJ/mol)	$-\Delta H_a$ (kJ/mol)	ΔS_a (J/mol)
HCl	Without inhibitor	50.82	48.47	304.14
	With inhibitor	56.23	53.87	312.61
H_2SO_4	Without inhibitor	29.91	27.56	235.83
	With inhibitor	41.27	38.91	265.5

O. Radovico [18] proposes a classification of inhibitors based on the comparison of the activation energies obtained in their presence (E_a') or not (E_a). He distinguishes:

Inhibitors for which $E_a' > E_a$ adsorb on the substrate by electrostatic bonds (physisorption). Inhibitors for which $E_a' < E_a$ show an increase in protective power with temperature. They adsorb by strong bonds (chemisorption).

Inhibitors for which $E_a' = E_a$ show no change in protective power.

The activation energy (E_a) values were found to be higher in the presence of the Schiff base compared to those in acid solutions alone. This suggests that the Schiff base is physisorbed onto the steel surface. The activation enthalpy values were negative, indicating an exothermic dissolution process for XC48 steel. The high and negative values of entropy (ΔS_a) suggest a decrease in disorder during the transformation of reactants into activated iron-molecule complexes in the solution.

The inhibition of metal corrosion by organic compounds is generally explained by their adsorption onto the metal surface. This adsorption can be categorized as either physical

adsorption or chemisorption. The type of adsorption depends on various factors, including the charge of the metal, its structure, the chemical structure of the organic compound, and the nature of the electrolyte.

Chemisorption typically involves a transfer or sharing of electrons between the inhibitor molecules and the vacant d orbitals of the metal surface, leading to the formation of coordination bonds. This electron transfer often occurs with organic molecules containing multiple bonds or aromatic nuclei with π electrons.

Organic inhibitors usually possess at least one functional group that is considered active for chemisorption. In aromatic compounds, the introduction of a substituent can influence the electron density, thereby impacting the corrosion inhibiting efficiency. Electron-donating substituents generally increase the efficiency, while electron-withdrawing substituents tend to decrease it.

The surface coverage (θ) for different concentrations of the inhibitor in acidic medium is evaluated by the polarization curves using equation (6). This equation for calculating the degree of surface coverage with an inhibitor (BMDDM) is used, based on the assumption this inhibitor exhibits a predominantly blocking mechanism of action.

$$\theta = \frac{i_{\text{corr}} - i_{\text{corr,inh}}}{i_{\text{corr}}} \tag{6}$$

where i_{corr} and $i_{\text{corr,inh}}$ represent the corrosion current densities determined by extrapolating the Tafel lines after immersion in the acidic medium without and with the inhibitor, respectively.

In this study, different isotherms including Langmuir, Temkin and Frumkin were tested in order to find the suitable adsorption isotherm (Figures 8, 9 and 10).

According to these isotherms, the recovery rate (θ) is related to the inhibitor concentration *C* by the following equations:

$$\frac{C}{\theta} = \frac{1}{K_{\text{ads}}} + C \tag{7}$$ (Langmuir adsorption isotherm)

$$\exp(-2a\theta) = KC_{\text{inh}} \tag{8}$$ (Temkin adsorption isotherm)

$$\left(\frac{\theta}{1-\theta}\right)\exp(-2a\theta) = KC_{\text{inh}} \tag{9}$$ (Frumkin adsorption isotherm)

where *a* is an interaction constant between adsorbed particles; *C* is the concentration of the inhibitor in the solution; *K* is the equilibrium constant of the adsorption process.

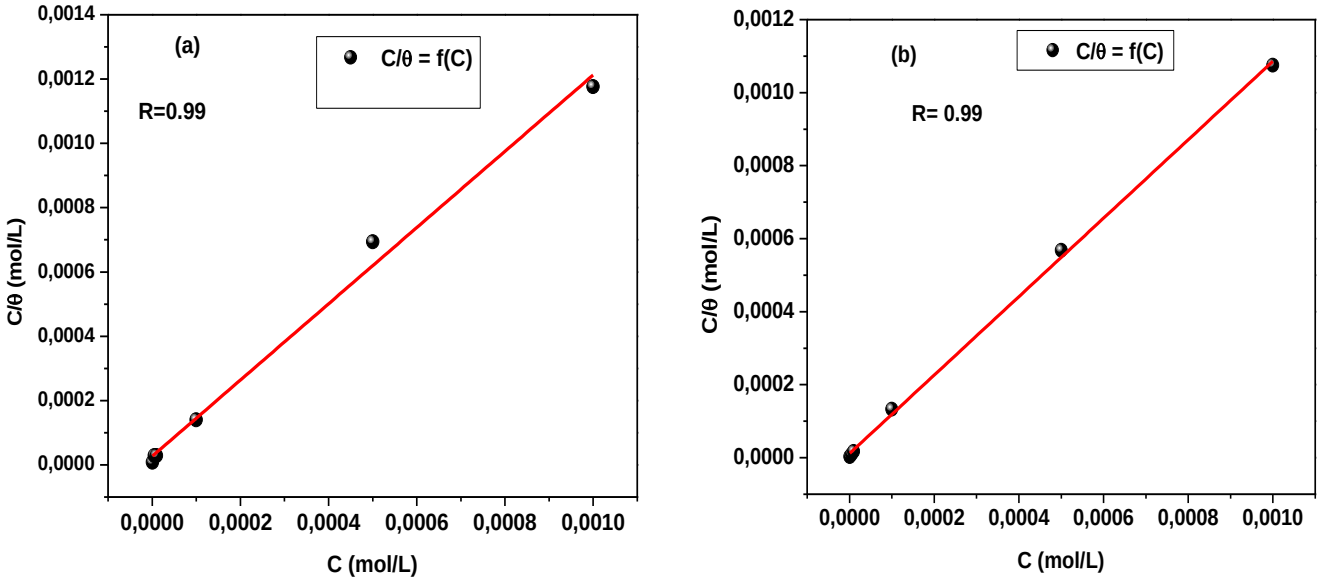

Figure 8. Langmuir adsorption isotherm of XC48 steel in both (a) 1 M HCl and (b) 0.5 M H_2SO_4 media in the presence of the Schiff base at room temperature.

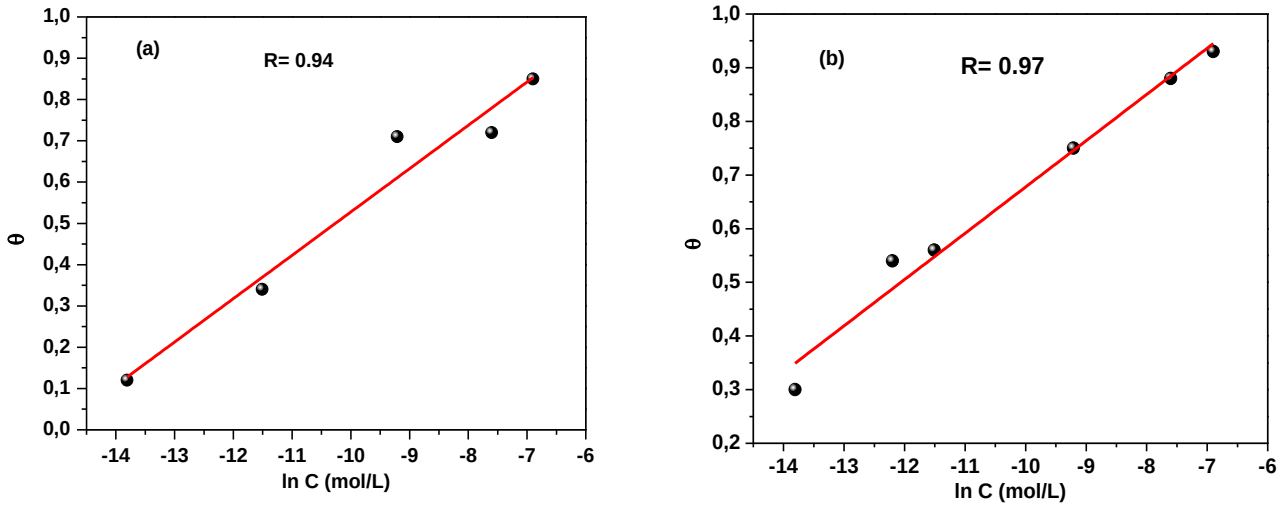

Figure 9. Temkin adsorption isotherm of XC48 steel (a) in 1 M HCl and (b) in 0.5 M H_2SO_4 media in the presence of the Schiff base at room temperature.

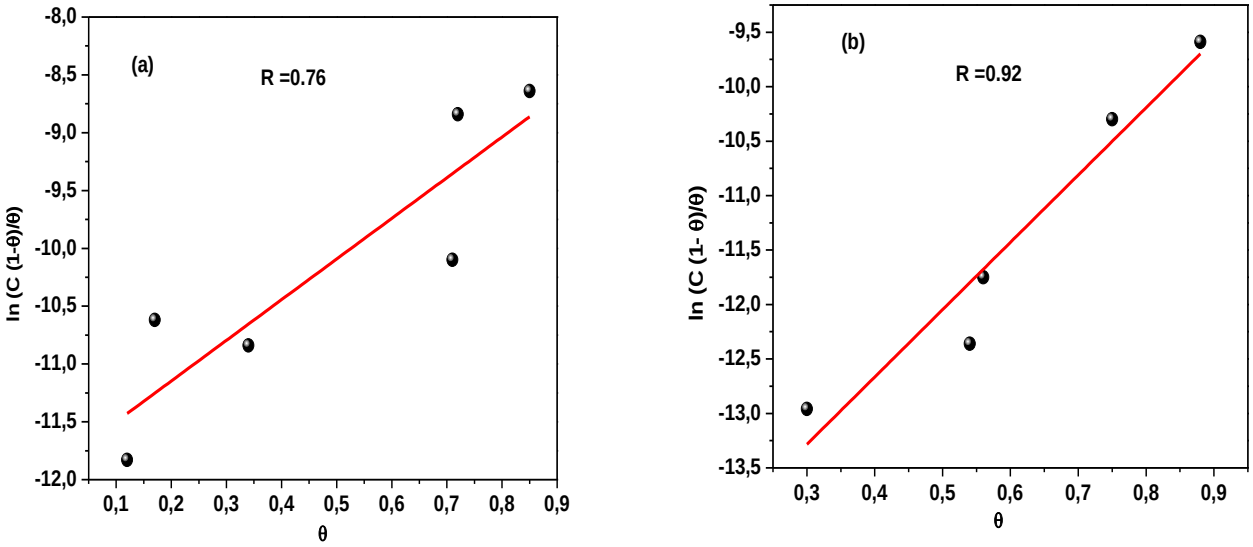

Figure 10. Frumkin adsorption isotherm of XC48 steel in both (a) 1 M HCl and (b) 0.5 M H_2SO_4 media in the presence of the Schiff base at room temperature.

It appears that the best fit was obtained with the Langmuir isotherm. From the plot of C_{inh}/θ as a function of C_{inh} (Figure 16), the value of K_{ads} is determined from the intersection with the C_{inh}/θ axis. The value of K_{ads} is equal to $1.36 \cdot 10^5$ M in 1 M HCl medium and $4.28 \cdot 10^5$ M in 0.5 M H_2SO_4 medium. The value of the free energy ΔG^0_{ads} for the inhibitor is calculated from equation (10):

$$\Delta G^0_{ads} = -RT \ln(55.55 K_{ads}) \quad (10)$$

where R is the universal gas constant, T is the temperature and the value 55.5 in the above equation is the concentration of water in the solution expressed in mol/l. The negative value of ΔG^0_{ads} indicates the spontaneity of the adsorption process and the stability of the double layer adsorbed on the metal surface. Generally, ΔG^0_{ads} values close to –20 kJ/mol or lower are related to electrostatic interactions between the negatively charged molecules and the positively charged metal (physical adsorption), while those close to –40 kJ/mol or higher imply a charge transfer between the organic molecules and the metal surface (chemisorption) [19–22]. In this work, the calculated ΔG^0_{ads} values are –35.71 and –38.29 kJ/mol in hydrochloric acid and sulfuric acid respectively which shows that this inhibitor is physisorbed and chemisorbed on the metal surface. The spontaneity of the adsorption process and the stability of the adsorbed layer on the metal surface are confirmed by the negative ΔG^0_{ads} values [14].

3.2. Morphological study by scanning electron microscopy (SEM)

In order to characterize the surface condition of X48 carbon steel before and after immersion in two different media, 1 M HCl and 0.5 M H_2SO_4 in the absence and presence of 10^{-3} M of

BMDDM synthesized, we used a scanning electron microscope (SEM). We carried out a systematic observation of the samples by comparing the surface condition between the sample that had not undergone any attack and those treated. Surface condition of X48 carbon steel after polishing with abrasive paper at different grain sizes is shown in Figure 11(a). The clean and well-polished surface shows no signs of deterioration.

The morphologies of corrosion attack in the absence and presence of 10^{-3} M of synthesized inhibitor after 24 h of immersion are presented in Figures 11(b–e).

Indeed, we notice on the images of the steel surface after 24 h of immersion in 1 M HCl alone and H_2SO_4 alone (Figures 11(b, d)) black spots corresponding to corrosion pits as well as gray and white areas which correspond to the formation of corrosion products [23, 24]. This clearly confirms that the steel has undergone corrosion in the absence of inhibitor. On the other hand, in the presence of 10^{-3} M of BMDDM, we observe on the micrographs of the surface of carbon steel X48 after 24 h of immersion in 1 M HCl medium and in H_2SO_4 medium (Figures 11(c, e)) that the surface is covered with a protective film [25, 26]. We see that the surface is covered with a product reflecting the presence of an organic product. This clearly shows that the inhibition is due to the formation, by adsorption of organic molecules, of a stable and insoluble protective deposit on the surface of the X48 carbon steel which slows down the corrosion process in the corrosive solution.

4. Conclusion

This work has made it possible to meet the objectives set concerning the inhibitor against corrosion of XC48 steel by BMDDM adsorption in two different media, 1 M hydrochloric acid and 0.5 M sulfuric acid. The evaluation of the inhibitory properties of BMDDM was carried out by stationary (potentiodynamic polarization) and transient (electrochemical impedance spectroscopy) electrochemical methods. The inhibitory efficiency reached 89.33% in 1 M hydrochloric acid medium and 88.37% in 0.5 M sulfuric acid medium for an optimal concentration of 10^{-3} M. The results obtained revealed that the inhibitor of the studied Schiff base is mixed. The inhibition mechanism obeys the Langmuir isotherm in both HCl and H_2SO_4 acids. The ΔG_{ads} values calculated in both HCl and H_2SO_4 media indicate that both compounds are chemisorbed and physisorbed. In terms of temperature, the maximum inhibitory efficiency is 78.45% at a temperature of 40°C in a hydrochloric medium, and 76.05% at a temperature of 30°C in a sulfuric acid medium. Several issues are still open for future investigation in order to fully understand the corrosion of steels and their inhibition in the various solutions encountered in the industrial sector. Hopefully, the results presented in this study gives a contribution to this understanding.

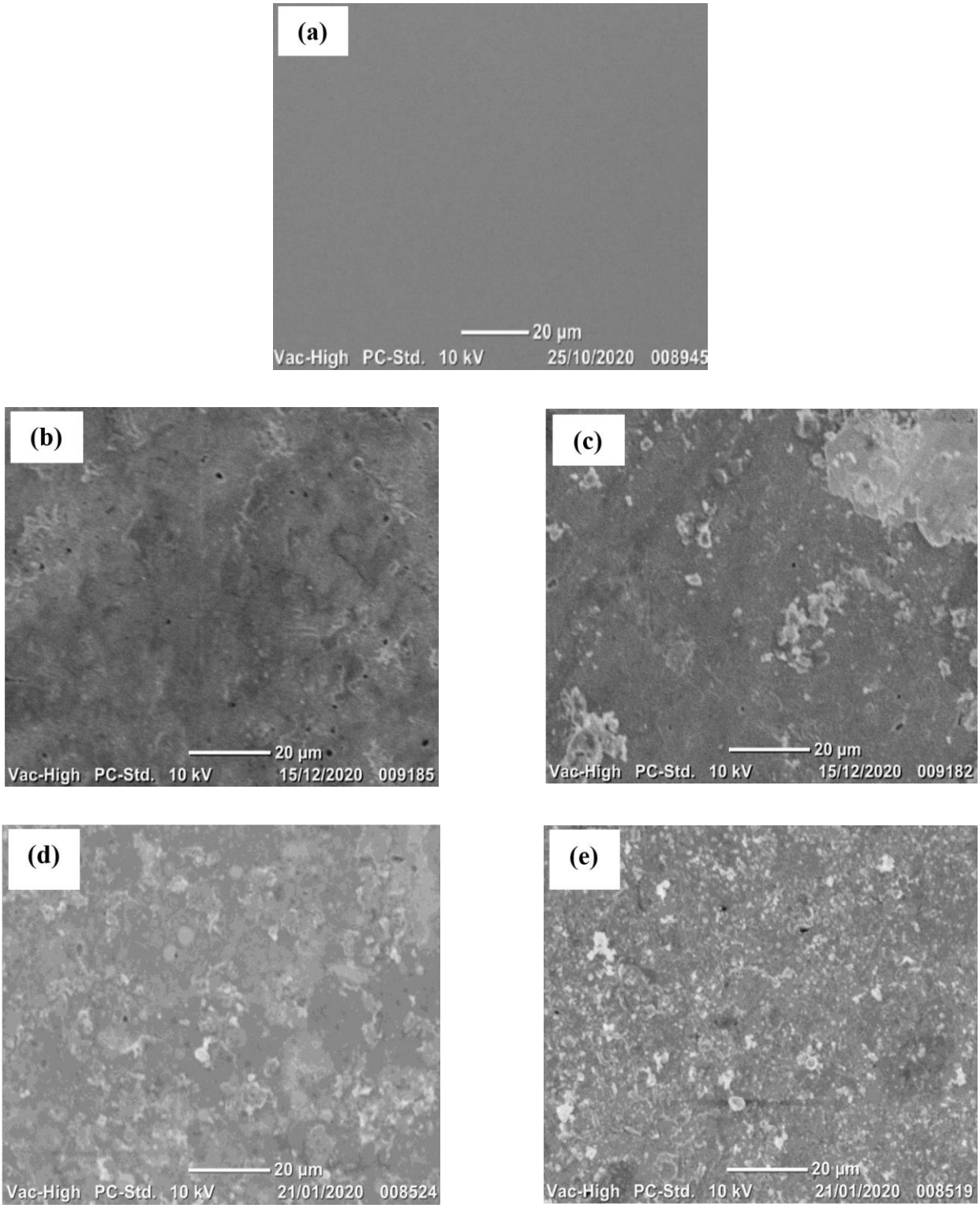

Figure 11. Micrographs (SEM): (a) of the surface of carbon steel X48, (b): after 24 h of immersion in HCl alone, (c) after 24 h of immersion in HCl in the presence of 10^{-3} M of BMDDM, (d): after 24 h of immersion in H_2SO_4 alone, (e) after 24 h of immersion in H_2SO_4 in the presence of 10^{-3} M of BMDDM.

References

1. S. Pal, M. Chaudhary, P. Jain, P. Singh, A.K. Yadav, S.K. Singh and I. Bahadur, Chapter 9 – An involvement of ionic liquids and other small molecules as promising corrosion inhibitors in recent advancement of technologies in chemical industries, *Adv. Appl. Ionic Liq*., 2023, 223–245. doi: 10.1016/B978-0-323-99921-2.00004-5
2. A.H. Khalaf, Y. Xiao, N. Xu, B. Wu, H. Li, B. Lin, Z. Nie and J. Tang, Emerging AI technologies for corrosion monitoring in oil and gas industry: A comprehensive review, *Eng. Fail. Anal*., 2024, **155**, 107735. doi: 10.1016/j.engfailanal.2023.107735
3. F. Belalia, A. Harichane, D. Belfennache, R. Yekhlef, S. Zaiou, M. Hemdan and M.A. Ali, Elimination of Inorganic Pollutants Using a Novel Biomaterial Adsorbent, *Egypt. J. Chem*., 2024, **67**, no. 13, 1167–1176. doi: 10.21608/ejchem.2024.280399.9541
4. S. Sarkar, S. Zamindar, M. Murmu, S. Mandal, G. Majumdar and P. Banerjee, 8.20 – Importance of corrosion inhibition in oil and gas industries: Environmental health and safety for sustainable development of oil as well as gas industries, *Comprehensive Materials Processing (Second Edition)*, 2024, **8**, 272–281. doi: 10.1016/B978-0-323-96020-5.00102-3
5. Y. Liu, Y. Zhou, W. Wang, L. Tian, J. Zhao and J. Sun, Synergistic damage mechanisms of high-temperature metal corrosion in marine environments: A review, *Prog. Org. Coat*., 2024, **197**, 108765. doi: 10.1016/j.porgcoat.2024.108765
6. S.A. Al Kiey, A.A. El-Sayed and A.M. Khalil, Controlling corrosion protection of mild steel in acidic environment *via* environmentally benign organic inhibitor, *Colloids Surf. A*, 2024, **683**, 133089. doi: 10.1016/j.colsurfa.2023.133089
7. O.A. Mohsen, M.W. Faraj, T.M. Darwesh, N.H. Jawad, K.M. Abed, A. Hayyan, Y.M. Alanazi, J. Saleh, B.S. Gupta, M. Zulhaziman and M. Salleh, Indole derivatives efficacy and kinetics for inhibiting carbon steel corrosion in sulfuric acid media, *Results Eng*., 2024, **23**, 102755. doi: 10.1016/j.rineng.2024.102755
8. E. Ech-chihbi, B. Es-Sounni, C. Kerdoune, A. Mouhib, M. Bakhouch, R. Salim, R. Salghi, B. Hammouti, N. Mazoir, M. Chafiq, A. Chaouiki and Y.G. Ko, Corrosion inhibition performance and adsorption mechanism of new synthesized symmetrical diarylidenacetone-based inhibitor on C38 steel in 15 % HCl medium: Theoretical insight and experimental validation, *Colloids Surf. A*, 2024, **702**, 135073. doi: 10.1016/j.colsurfa.2024.135073
9. U. Mamudu, J.H. Santos, S.A. Umoren, M.S. Alnarabiji and R.C. Lim, Investigations of corrosion inhibition of ethanolic extract of *Dillenia suffruticosa* leaves as a green corrosion inhibitor of mild steel in hydrochloric acid medium, *Corros. Commun*., 2024, **15**, 52–62. doi: 10.1016/j.corcom.2023.10.005
10. K.M. Shwetha, B.M. Praveen and B.K. Devendra, A review on corrosion inhibitors: Types, mechanisms, electrochemical analysis, corrosion rate and efficiency of corrosion inhibitors on mild steel in an acidic environment, *Res. Surf. Interfaces*, 2024, **16**, 100258. doi: 10.1016/j.rsurfi.2024.100258

11. M. Li, D. Zhang, R. Zhang, F. Wang, Y. Song, F. Chen, J. Yang and C. Li, Recent advances in the unlined cast iron pipe scale characteristics, cleaning techniques and harmless disposal methods: An overview, *Chemosphere*, 2023, **340**, 139849. doi: 10.1016/j.chemosphere.2023.139849
12. A. Singh, K.R. Ansari, I.H. Ali, N.R. Sharma, A. Bansal, A.K. Alanazi, M. Younas, A.H. Alamri, Y. Lin and A. Noureldeen, Corrosion and bacterial growth inhibition by amino acid functionalized pyridine derivative at P110 steel/oil formation water interface: Experimental, surface and molecular docking investigations, *J. Mol. Liq*., 2023, **391**, 123305. doi: 10.1016/j.molliq.2023.123305
13. J. Liu, M. Hang, M. Jiang, G. Xu and H. Song, Corrosion inhibition performance and mechanism of triethanolamine-triisopropanolamine rust inhibitor in the simulated concrete pore solution, *J. Build. Eng*., 2024, **96**, 110551. doi: 10.1016/j.jobe.2024.110551
14. L. Toukal, D. Belfennache, M. Foudia, R. Yekhlef, F. Benghanem, B. Hafez, H. Elmsellem and I. Abdel-Rahman. Inhibitory power of *N*,*N*′-(1,4-phenylene)bis(1-(4-nitrophenyl) methanimine) and the effect of the addition of potassium iodide on the corrosion inhibition of XC70 steel in HCl medium: Theoretical and experimental studies. *Int. J. Corros. Scale Inhib*., 2022, **11**, no. 1, 438–464. doi: 10.17675/2305-6894-2022-11-1-26
15. S. Brioua, A. Delimi, H. Ferkous, S. Boukerche, H. Allal, A. Boublia, A. Djedouani, M. Berredjem, A. Kahlouche, K.O. Rachedi, A. Abdennouri, M. Alam, B. Ernst and Y. Benguerba, Enhancing corrosion resistance of XC38 steel using sulfur and nitrogen-containing phenyl thiosemicarbazone: A comprehensive experimental and computational analysis, *J. Taiwan Inst. Chem. Eng*., 2024, **165**, 105718. doi: 10.1016/j.jtice.2024.105718
16. A.A. Altalhi, Novel *N*-heterocyclic Schiff base based on Isatin derivative as a sustainable, eco-friendly, and highly efficiency corrosion inhibitor for carbon steel in sulfuric acid medium: Electrochemical and Computational investigation, *Int. J. Electrochem. Sci*., 2024, **19**, no. 1, 100449. doi: 10.1016/j.ijoes.2023.100449
17. M.S. Al-Sharif, Electrochemical and theoretical assessment of two heterocyclic Schiff bases as effective corrosion inhibitors for carbon steel in sulfuric acid solution, *Int. J. Electrochem. Sci*., 2024, **19**, no. 2, 100454. doi: 10.1016/j.ijoes.2023.100454
18. O. Radovico, *Proceedings of The 7th European Symposium on Corrosion Inhibitors*, European Federation of Corrosion, Italy, 1990, p. 330.
19. D. Zhang, Y. Tang, S. Qi, D. Dong, H. Cang and G. Luc, The inhibition performance of long-chain alkyl-substituted benzimidazole derivatives for corrosion of mild steel in HCl, *Corros. Sci*., 2016, **102**, 517–622. doi: 10.1016/j.corsci.2015.10.002
20. X. Wang, Y. Wan, Y. Zeng and Y. Gu, Investigation of Benzimidazole Compound as a Novel Corrosion Inhibitor for Mild Steel in Hydrochloric Acid Solution, *Int. J. Electrochem. Sci*., 2012, **7**, no. 3, 2403–2415. doi: 10.1016/S1452-3981(23)13888-0

21. A. Dutta, S.S. Panja, M.M. Nandi and D. Sukul, Effect of Optimized Structure and Electronic Properties of Some Benzimidazole Derivatives on Corrosion Inhibition of Mild Steel in Hydrochloric Acid Medium: Electrochemical and Theoretical Studies, *J. Chem. Sci*., 2015, **127**, 921–929. doi: 10.1007/s12039-015-0850-x
22. Z. Salarvand, M. Amirnasr, M. Talebian, K. Raeissi and S. Meghdadi, Enhanced corrosion resistance of mild steel in 1 M HCl solution by trace amount of 2-phenyl-benzothiazole derivatives: Experimental, quantum chemical calculations and molecular dynamics (MD) simulation studies, *Corros. Sci*., 2017, **114**, 133–145. doi: 10.1016/j.corsci.2016.11.002
23. A. Chaouiki, H. Lgazc, R. Salghib, M. Chafiq, H. Oudda, Shubhalaxmi, K.S. Bhat, I. Cretescu, I.H. Ali, R. Marzouki and I.-M. Chang, Assessing the impact of electron-donating-substituted chalcones on inhibition of mild steel corrosion in HCl solution: Experimental results and molecular-level insights Chung, *Colloids Surf. A*, 2020, **588**, 124366. doi: 10.1016/j.colsurfa.2019.124366
24. R.S. Erami, M. Amirnasra, S. Meghdadi, M. Talebian, H. Farrokhpour and K. Raeissi, Carboxamide derivatives as new corrosion inhibitors for mild steel protection in hydrochloric acid solution, *Corros. Sci*., 2019, **151**, 190–197. doi: 10.1016/j.corsci.2019.02.019
25. F. Boudjellal, H.B. Ouici, A. Guendouzi, O. Benali and A. Sehmi, Experimental and theoretical approach to the corrosion inhibition of mild steel in acid medium by a newly synthesized pyrazole carbothioamide heterocycle, *J. Mol. Struct*., 2020, **1199**, 127051. doi: 10.1016/j.molstruc.2019.127051
26. H. Lgaz, S.K. Saha, A. Chaouiki, K.S. Bhat, R. Salghi, Shubhalaxmi, P. Banerjee, I.H. Ali, M.I. Khan and I.-M. Chung, Exploring the potential role of pyrazoline derivatives in corrosion inhibition of mild steel in hydrochloric acid solution: Insights from experimental and computational studies, *Constr. Build. Mater*., 2020, **233**, 117320. doi: 10.1016/j.conbuildmat.2019.117320

♦ ♦ ♦